REVIEW OF SCIENTIFIC INSTRUMENTS VOLUME 74, NUMBER 7 JULY 2003

Measurement of oxygen atom density employing vacuum ultraviolet absorption spectroscopy with microdischarge hollow cathode lamp

Hisao Nagai[a)]
Department of Quantum Engineering, Nagoya University, Furo-cho, Chikusa-ku, Nagoya 464-8603, Japan

Mineo Hiramatsu
Department of Electrical and Electronic Engineering, Meijo University, 1-501 Shiogamaguchi, Tempaku-ku, Nagoya 468-8502, Japan

Masaru Hori[b)] and Toshio Goto
Department of Quantum Engineering, Nagoya University, Furo-cho, Chikusa-ku, Nagoya 464-8603, Japan

(Received 17 December 2002; accepted 4 April 2003)

The compact measurement system for absolute density of oxygen (O) atom has been developed, which employs a vacuum ultraviolet absorption spectroscopy (VUVAS) technique with a high-pressure microdischarge hollow cathode lamp (MHCL) as a light source. The influences of self-absorption, emission line profile of the MHCL, and background absorption of oxygen molecule (O_2) on the determination of absolute O atom density were taken into consideration. This system has been applied for measuring absolute O atom densities in an inductively coupled O_2 plasma. O atom densities were estimated to be on the order of $1\times10^{12}-1\times10^{13}\,\mathrm{cm}^{-3}$ at an input power of 100 W and an O_2 pressure ranging from 1.3 to 26.7 Pa. The behavior of O atom density measured using VUVAS technique was consistent with that obtained by actinometry technique using O emission intensities of 844.6 nm and 777.4 nm lines. Moreover, the lifetime of O atom in the afterglow plasma has been measured. The decay curves of the O atom density were fitted with exponential functions. The extinction process of O atom in the inductively coupled O_2 plasma has been discussed. © *2003 American Institute of Physics.* [DOI: 10.1063/1.1582386]

I. INTRODUCTION

Oxygen-based plasmas have been extensively used for the material processing in oxidation of materials, chamber cleaning, organic polymer etching.[1–3] In the case of the formation of ultrathin dielectric films such as a gate oxide film, the low-temperature oxidation process is highly desirable, compared with the conventional thermal oxidation of silicon. For this purpose, the plasma oxidation method is successfully employed.[4,5] Instead of using the thermal energy, the plasma oxidation utilizes a highly activated oxygen plasma, which includes a large amount of reactive oxygen (O) atoms in the ground state, excited O atoms, O ionic species, and vibrationally excited oxygen molecules (O_2). From the viewpoint of developing the oxidation processes used in the next generation, quantitative studies on the behavior of O atoms in the plasma should be dedicated to the clarification of the reaction mechanism of O atoms in gas phase as well as on the surface, and the *in situ* monitoring system of absolute O atom density in the processing plasmas is strongly required. Moreover, measurement of the loss rate of O atoms in afterglow plasma enables us to clarify the reaction mechanism of O atom. The knowledge of loss kinetics of O atoms is indispensable for clarifying and controlling the surface reactions of O atoms. The value of the surface loss probability is much useful for modeling and simulation of plasmas as well.

So far, measurements of O atom density have been carried out by titration,[6] actinometry,[7,8] two-photon laser-induced fluorescence spectroscopy,[9–13] and absorption spectroscopy.[14] The titration method is performed in the downstream rather than in the plasma and thus has errors due to postdischarge recombination. Actinometry is a simple technique which can give relative density changes in the plasma. Two-photon absorption laser-induced fluorescence spectroscopy (TALIF) is an *in situ* technique, and has excellent spatial and temporal resolution compared with the other methods. However, the applicable condition is restricted for this method, and these outstanding features are not fulfilled in most cases. The system of TALIF is rather complex and expensive, and the calibration is necessary for obtaining the absolute density. On the other hand, absorption spectroscopy is an *in situ* method and is possibly applied to absolute density measurement for the various kinds of species with ease.

Recently, our group has developed a measurement system of absolute densities of hydrogen and nitrogen atoms using vacuum ultraviolet absorption spectroscopy (VUVAS) with microdischarge hollow cathode lamp (MHCL).[15,16] The size of the hollow cathode was as small as 0.1 mm in diameter, resulting in a high current density in the cathode, which is favorable for attaining high dissociation degree of gases and obtaining spectral emission. Moreover, since the MHCL was compact (80×80×160 mm), the system for measuring

[a)]Author to whom correspondence should be addressed; electronic mail: h-nagai@nuee.nagoya-u.ac.jp
[b)]Electronic mail: hori@nuee.nagoya-u.ac.jp

Downloaded 29 Oct 2006 to 133.6.32.11. Redistribution subject to AIP license or copyright, see http://rsi.aip.org/rsi/copyright.jsp

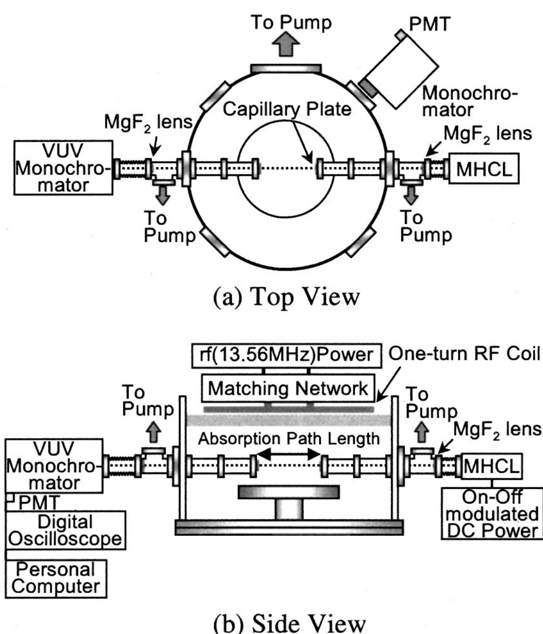

FIG. 1. Schematic diagram of ICP reactor equipped with VUVAS system employing MHCL: (a) top view and (b) side view.

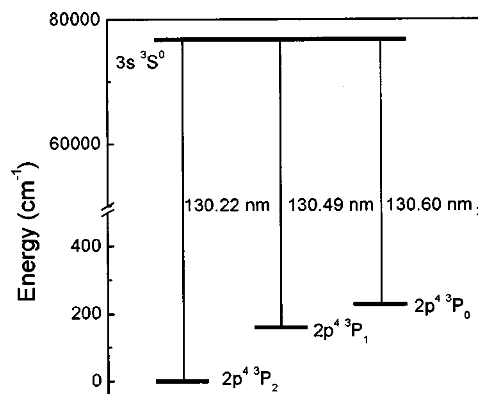

FIG. 2. The partial energy level diagram of O atom used this study.

atom density can be easily installed to the process chamber. Therefore, the VUVAS system with MHCL could be applied to evaluate the behavior of radicals in processing plasmas.[17,18]

On the other hand, since the energy of photons used in the VUVAS technique is high (10 eV), it has been reported that the background absorption due to parent gases and species produced by plasmas would occur in the plasmas using reactive gases such as hydrocarbon and fluorocarbons.[19,20] The background absorption has a strong influence on the determination of the density of species in the case of the measurements using absorption spectroscopy. In order to measure the absolute O atom density in reactive plasmas with high accuracy, it is important to assess the influence of the background absorption on the absorption by O atoms.

In this study, we have established a measurement system of O atom density using VUVAS technique employing the MHCL. The influences of self-absorption and emission line profile of O_2 MHCL were evaluated. This system has been applied to the determination of absolute O atom densities in an O_2 inductively coupled plasma (ICP). Moreover, the lifetime of O atom in the afterglow plasma has been measured and the extinction process of O atom has been discussed.

II. EXPERIMENT

Figure 1 shows a schematic diagram of ICP reactor equipped with VUVAS system employing MHCL. The ICP chamber was made with stainless steel of 50 cm in diameter and 30 cm in height. A one-turn coil antenna with a diameter of 30 cm was set on the quartz window at the top of the chamber. A radio-frequency (rf) voltage operating at 13.56 MHz was applied to the one-turn coil antenna. The MHCL was used as a vacuum ultraviolet (VUV) light source for absorption spectroscopy. Detailed structure of the MHCL was described in Ref. 15. The O_2 MHCL was operated at a total pressure of 1 atm and a discharge current of 10 mA. O_2 gas was diluted by helium (He) in the O_2 MHCL. The VUV light from MHCL was made parallel by the MgF_2 lens and introduced into the process chamber. The absorption path length was restricted to be 12.6 cm by using two stainless steel pipes and the capillary plate in order to prevent the saturation of absorption. The VUV light passing through the plasma was focused on the slit of a VUV monochromator (Acton Research Corp., ARC VM-520) by the MgF_2 lens and detected by a photomultiplier tube. The signal was averaged by a digital oscilloscope and recorded with a personal computer.

Figure 2 shows the partial energy level diagram of O atom. The ground state $2p^4\,^3P_J$ is composed of three sublevels $(J=1,2,3)$. The transition lines of O atom used for the absorption measurements were $3\,s\,^3S^0-2p^4\,^3P_2$ at 130.217 nm, $3\,s\,^3S^0-2p^4\,^3P_1$ 130.487 nm, and $3\,s\,^3S^0-2p^4\,^3P_0$ 130.604 nm of O atom as shown in Fig. 2. The inlet slit width of the VUV monochromator was set to 100 μm, and the wavelength resolution was within 0.4 nm. Therefore, in this study, we measured the total absorption intensity for three transition lines $(^3S^0-^3P_0, ^3S^0-^3P_1, ^3S^0-^3P_2)$ of O atoms.

III. RESULTS AND DISCUSSION

A. Background absorption

The broad background absorption profiles due to parent gases and species produced in the plasma are generally observed. Absorptions around 130 nm by parent O_2 molecules without plasma were examined using some emission lines around 130 nm employing MHCL with different gases as a light source. Figure 3 shows the fraction of absorptions around 130 nm as a function of O_2 pressure in process chamber without plasma. As the O_2 pressure increased, the fraction of absorptions around 130 nm increased. This fact indicated that the O_2 molecule absorbed the VUV light around 130 nm. The absorptions using the N line at 124.3 nm and the C line at 132.9 nm were larger than that using the O line at 130.2 nm, since there are strongly absorbed by the Schumann–Runge system[21] at 130–170 nm and by two intense maxima at 124.3 and 124.4 nm for the O_2 molecule.[22] Therefore, these two lines were not adequate to be used as a reference of background absorption. The absorptions using O line at 130.2 nm and H_2 broad peak at 128.5 nm showed

Downloaded 29 Oct 2006 to 133.6.32.11. Redistribution subject to AIP license or copyright, see http://rsi.aip.org/rsi/copyright.jsp

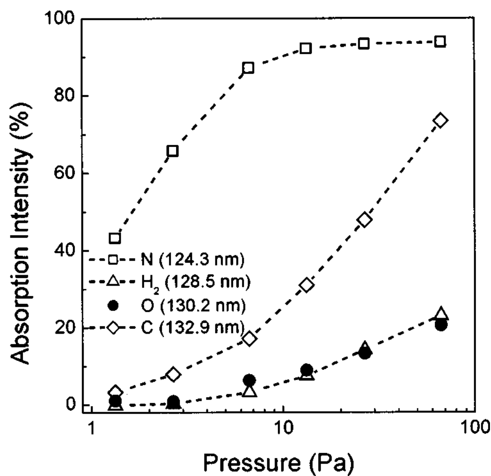

FIG. 3. The fraction of absorptions around 130 nm as a function of O_2 pressure in process chamber without plasma.

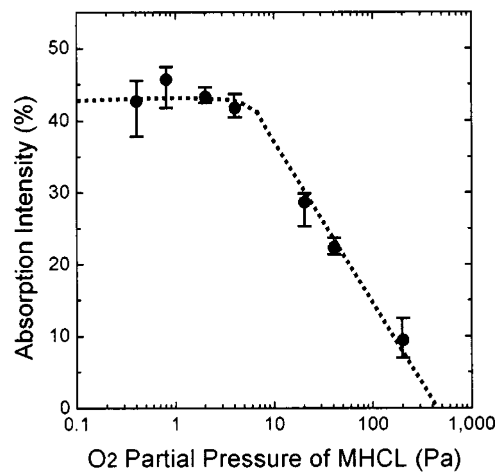

FIG. 4. The absorption intensity around 130 nm in an inductively coupled O_2 plasma at pressure of 2.7 Pa, a total flow rate of 100 sccm, and rf power of 200 W as a function of the O_2 partial pressure in the O_2 MHCL.

similar behavior in the pressure range from 1.33 to 66.7 Pa. Consequently, we used the H_2 broad peak in order to measure the background absorption at the O line.

When the background absorption is present, the absorption I_A measured at 130.2 nm is given by

$$I_A = \frac{\sum_{x=1}^{3} \int a_x f_1(\nu)[1-\exp\{-a_x k_0 f_2(\nu) - k_{\mathrm{BA}}\}L] d\nu}{\sum_{x=1}^{3} \int a_x f_1(\nu) d\nu}, \tag{1}$$

where ν is the spectral frequency, a_x $(x=1-3)$ are the ratio of relative intensities of the ${}^3S^0-{}^3P_0$, ${}^3S^0-{}^3P_1$, and ${}^3S^0-{}^3P_2$ lines, $f_1(\nu)$ is the emission-line profile of the light source, $f_2(\nu)$ is the absorption-line profile of the plasma to be measured, k_0 is the absorption coefficient at the center frequency due to the absorption of the O atom [so that $f_2(\nu)$ is normalized to unity at center frequency], k_{BA} is the absorption coefficient due to the background absorption, and L is the absorption path length. The value of k_{BA} is calculated using the following formula:

$$k_{\mathrm{BA}} = -\frac{1}{L}\ln(1-I_{\mathrm{BA}}), \tag{2}$$

where I_{BA} is the absorption coming from the background obtained employing the H_2 line at 128.5 nm, as explained above.

B. Characteristics of O_2 MHCL line profile

In order to estimate the self absorption in the O_2 MHCL, we have measured the absorption intensities around 130 nm in an inductively coupled O_2 plasma at a pressure of 2.7 Pa, a total flow rate of 100 sccm, and a rf power of 200 W. Figure 4 shows the absorption intensities around 130 nm in O_2 ICP as a function of O_2 partial pressure in the O_2 MHCL. The absorption intensity was almost constant in the O_2 partial pressure range up to 5.0 Pa. Then, the absorption intensity decreased with further increasing O_2 partial pressure in the O_2 MHCL. The self absorption in the lamp at high O_2 pressure resulted in the decrease of the absorption intensity because it preferentially weakens the line intensity at the center of the emission line profile where absorption is strong. Therefore, the results shown in Fig. 4 indicate that the distortion of the emission profile due to self absorption in the O_2 MHCL could be negligible when the O_2 partial pressure in the MHCL is below 5.0 Pa. The emission of the O line from the lamp operating at O_2 partial pressure of 5.0 Pa has an intensity level sufficient to be used as a light source for absorption measurements.

In order to estimate the O line emission profile of the O_2 MHCL, the absorption intensity due to inductively coupled O_2 plasma was measured as a function of rf power. The line profile can be determined by means of the comparison between the measured absorption intensity and the theoretical absorption intensity as a function of plasma optical thickness expressed by kL. The plasma optical thickness (or O atom density in the plasma) varies with the rf power. In this study, a small amount (1%) of Ar gas was added to O_2 gas in the process chamber and the Ar emission intensity at 750.4 nm was measured in order to estimate the plasma optical thickness. Here we assumed that the dissociation rate of O_2 molecules, that is the O atom density in the plasma, is proportional to the Ar emission intensity, since the pressure in the plasma is constant. Figure 5 shows the measured absorption

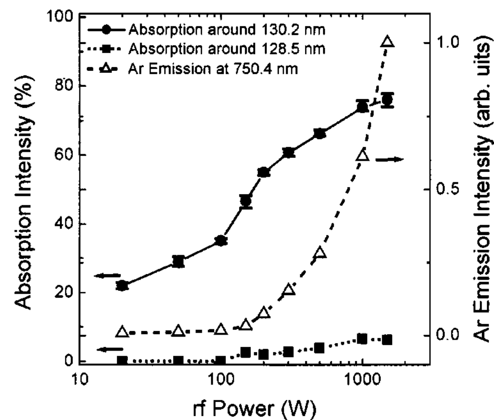

FIG. 5. The measured absorption intensities, the Ar emission intensity, and background absorption as a function of the rf power in probed plasma.

Downloaded 29 Oct 2006 to 133.6.32.11. Redistribution subject to AIP license or copyright, see http://rsi.aip.org/rsi/copyright.jsp

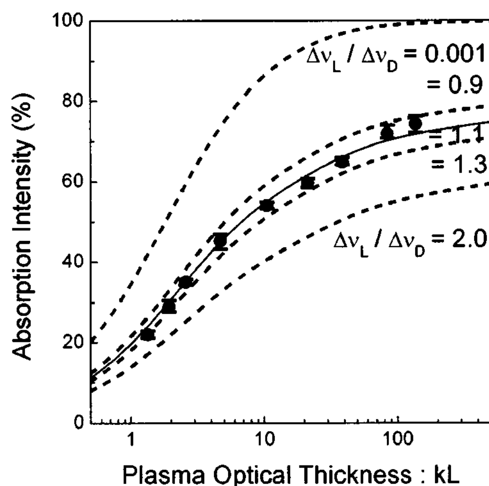

FIG. 6. Calculated average absorption intensity for O resonance lines as a function of plasma optical thickness for various values of $\Delta\nu_L/\Delta\nu_D$. The measured absorption intensity is plotted as a function of the plasma optical thickness, assuming that the Ar emission intensity is proportional to the plasma optical thickness.

intensities at 130.2 nm, the Ar emission intensity, and background absorption (measured using H_2 peak at 128.5 nm) as a function of rf power in the plasma. The measured plasma conditions were maintained at a total pressure of 2.6 Pa and a total flow rate of 100 sccm. The O_2 MHCL was operated at a total gas pressure of 1 atm, O_2 partial pressure of 5 Pa, and a discharge current of 10 mA; under this condition, the self absorption should be negligible as indicated in Fig. 4. Theoretical absorption intensity was calculated as follows. The emission intensities of the three lines from the O_2 MHCL are calculated from the transition probability A; that is, the ratio of relative intensities of the ${}^3S^0-{}^3P_0$, ${}^3S^0-{}^3P_1$, and ${}^3S^0-{}^3P_2$ lines is assumed to be 1, 0.618, and 0.195. Here, population of lower levels, and therefore, absorption coefficients at corresponding transitions, are assumed to follow Boltzmann distribution. The absorption profiles of O atom lines for the measured plasma are assumed to be Gaussian profiles corresponding to the O atom temperature of 300 K. The emission line profiles for O_2 MHCL are assumed to be Voigt profiles, because the O_2 MHCL is operating at high-pressure discharge (1 atm) and the Lorentz broadening is relatively large. The average absorption intensity for three O lines is evaluated for various values of $\Delta\nu_L/\Delta\nu_D$ in the Voigt profiles, where $\Delta\nu_L$ is the Lorentz and $\Delta\nu_D$ is the Doppler width. $\Delta\nu_D$ is determined by an O atom temperature of 300 K. Even if the fast excited O atoms with high temperature arising from dissociative excitation of O_2 molecules exist, they will be readily thermalized before they emit the light because of high-pressure discharge (about 1 atm). Figure 6 shows the calculated values of the average absorption intensity due to the three O transitions as a function of the plasma optical thickness, where the plasma optical thickness means the absorption coefficient multiplied by the absorption length. The absorption intensity taken into account the background absorption as shown in Fig. 5 is repotted as a function of the Ar emission intensity, where the proportionality constant between the Ar emission intensity and plasma optical thickness is chosen so that the data points closely fit one of the theoretical curves. As seen in Fig. 6, the points are well fitted by the theoretical curve $\Delta\nu_L/\Delta\nu_D = 1.1$. Thus, it is reasonable to assume that the O emission lines from O_2 MHCL have a Voigt profile with $\Delta\nu_L/\Delta\nu_D = 1.1$. We have estimated the influence of the temperature of the O atom on the estimation of absolute densities. Even if temperatures of the O atoms in measured plasmas and in the O_2 MHCL were as high as 1000 K, the calculated O atom densities do not change twice.

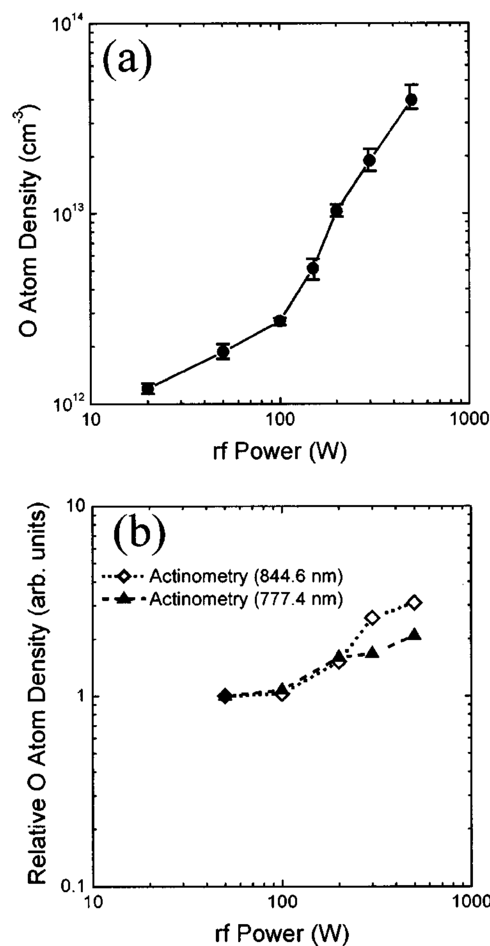

FIG. 7. (a) Absolute O atom density from VUVAS measurement and (b) relative O atom density obtained using actinometry technique as a function of the rf power at a pressure of 1.3 Pa and O_2 flow rate of 100 sccm.

C. Measurement of absolute O atom density

Using the VUVAS system employing the O_2 MHCL with the line profile parameter estimated above, we demonstrated the determination of absolute O atom density in inductively coupled O_2 plasmas. In addition, relative O atom density has been obtained using the actinometry technique. A small amount of argon (Ar) gas (1%) was added to the O_2 plasma. The relative O atom density was measured from the O emission intensities of 777.4 and 844.6 nm lines divided by normalized Ar emission line (750.4 nm) intensity (divided by Ar density).

Figures 7(a) and 7(b) show the absolute O atom density measured by VUVAS and relative O atom density obtained using the actinometry technique as a function of rf power at a pressure of 2.7 Pa, and O_2 flow rate of 100 sccm. As shown

Downloaded 29 Oct 2006 to 133.6.32.11. Redistribution subject to AIP license or copyright, see http://rsi.aip.org/rsi/copyright.jsp

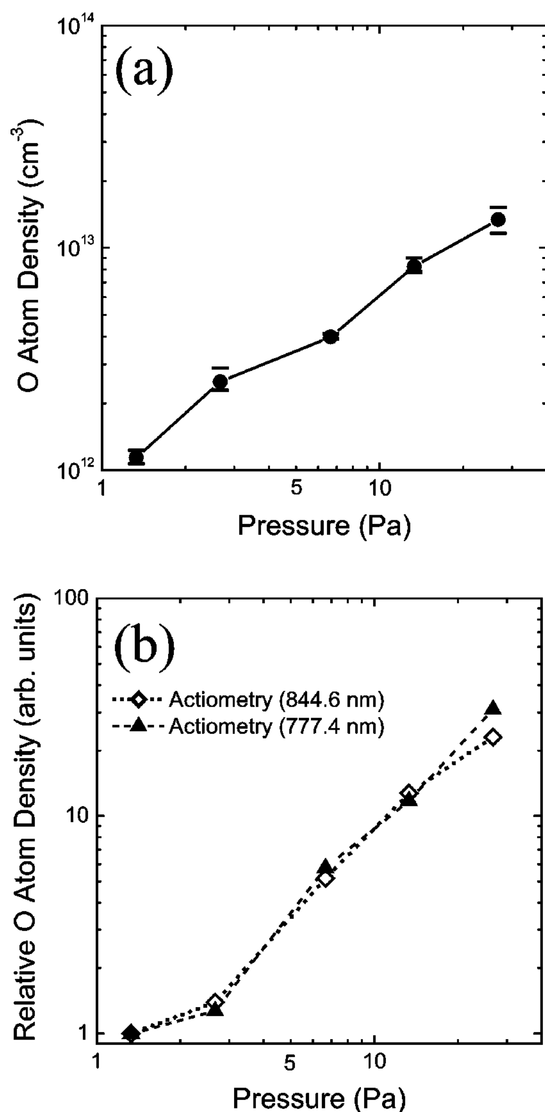

FIG. 8. (a) Absolute O atom density from VUVAS measurement and (b) relative O atom density obtained using actinometry technique as a function of total pressure at O_2 flow rate of 100 sccm and rf power of 100 W.

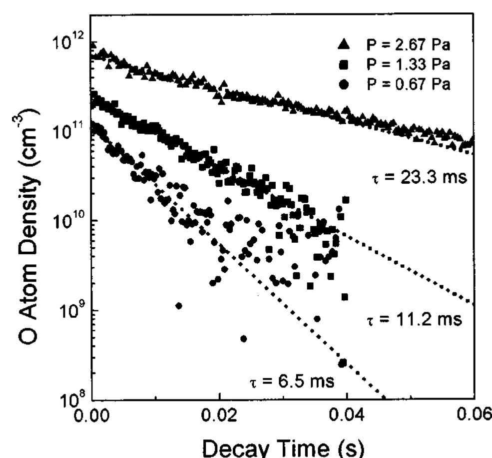

FIG. 9. Typical decay curves of O atom density in on–off modulated O_2 plasma at rf power of 50 W and O_2 flow rate of 100 sccm.

in Fig. 7(a), the absolute O atom density increased from 1×10^{12} to $4\times10^{13}\,cm^{-3}$ when the rf power increased from 20 to 500 W. The dissociation fraction is estimated to be about 6% at a rf power of 500 W. These absolute O atom densities measured in this study are equal to the O atom density measured by neutral mass spectrometry in an ICP reported previously elsewhere.[23] On the other hand, relative O atom densities obtained using 777.4 and 884.6 nm emission lines increased slowly with the increase of rf power as shown in Fig. 7(b). These two emission lines have different electron-impact excitation cross section of oxygen atom and excitation of oxygen atom by electron-impact dissociative excitation of molecular oxygen.[8] It is known that the O atom density obtained using the 884.6 nm emission line shows behavior of exact density rather than that obtained using the 777.4 nm emission line. However, the behavior of the absolute O atom density obtained from the actinometry technique using 844.6 nm, was consistent with that using 777.4 nm emission lines under our conditions. This consistency indicated that the generation of excited O atoms by means of electron-impact dissociative excitation of the O_2 molecule due to a high-energy electron would be small under our conditions. The behavior of the absolute O atom density determined using the VUVAS technique was also consistent with that obtained from the actinometry technique using 844.6 and 777.4 nm emission lines. However, the increase of O atom density determined using the VUVAS technique differs from that obtained from the actinometry technique using 844.6 and 777.4 nm emission lines. This tendency was reported in Ref. 24. This is because some assumptions of actinometry are not fulfilled under the condition of high rf power.

Figures 8(a) and 8(b) show the absolute O atom density measured by VUVAS and relative O atom density obtained using the actinometry technique as a function of total pressure in the process chamber at an O_2 flow rate of 100 sccm and rf power of 100 W. As shown in Fig. 8(a), the absolute O atom density increased from 1×10^{12} to $1\times10^{13}\,cm^{-3}$ when total pressure increased. The relative O atom density obtained using 777.4 nm and 884.6 nm emission lines also increased with the increase of total pressure as shown in Fig. 8(b). The behavior of absolute O atom density determined using the VUVAS technique was also consistent with that obtained from the actinometry technique using 844.6 and 777.4 nm emission lines.

D. Loss kinetics of O atoms in O_2 plasma afterglow

In order to clarify the loss kinetics of the O atom in O_2 plasma, the decay of the O atom density in the O_2 afterglow plasma was measured, and the surface loss probability of the O atom on the stainless-steel wall was estimated. Figure 9 shows typical decay curves of O atom densities in on–off modulated O_2 ICP at a pulsed rf power of 50 W (on period 33 ms, off period 67 ms), pressures of 0.67–6.67 Pa, and a flow rate of 100 sccm. These decay time measurements were carried out under the condition where the background absorption was not observed. As is apparent in Fig. 9, the decay curves of the O atom density measured at various pressures were well fitted with exponential functions, and the slope of the decay curve was steeper for the lower gas pressure.

Downloaded 29 Oct 2006 to 133.6.32.11. Redistribution subject to AIP license or copyright, see http://rsi.aip.org/rsi/copyright.jsp

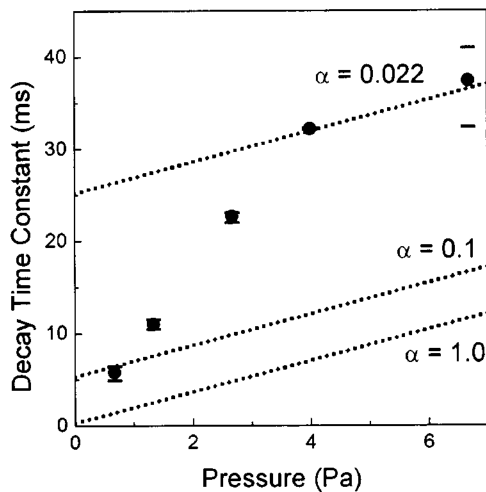

FIG. 10. The decay time constant of the O atom density as a function of pressure in O_2 plasma afterglow at rf power of 50 W and O_2 flow rate of 100 sccm.

Figure 10 shows the decay time constant of the O atom density as a function of pressure in O_2 afterglow plasma at a rf power of 50 W and an O_2 flow rate of 100 sccm. The decay time constant was increased with increasing O_2 pressure in the process chamber. Here, the loss mechanisms of the O atom have been discussed. The possible loss mechanisms for the O atom are the removal by pump action, the gas-phase recombination, and the diffusion followed by wall recombination. The residence time under our conditions was 230–2300 ms, and longer than the observed decay times. Therefore, the pump action can be dismissed as a possible loss mechanism. The relevant gas-phase reactions were taken into consideration

(I) $O+O+M \rightarrow O_2+M \quad k=2.1\times10^{-30}\ cm^6\,s^{-1}$,

(II) $O+O+O_2(^1\Delta) \rightarrow 2O_2 \quad k=7.4\times10^{-33}\ cm^6\,s^{-1}$,

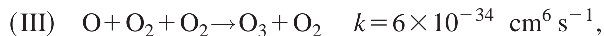

(III) $O+O_2+O_2 \rightarrow O_3+O_2 \quad k=6\times10^{-34}\ cm^6\,s^{-1}$,

(IV) $O+O_3 \rightarrow 2O_2 \quad k=9\times10^{-15}\ cm^3\,s^{-1}$.

These reaction constants are too small to account for the observed decay times (the O_3 density is taken to be 0.1% of total density).[10] Therefore, the gas-phase recombination could be dismissed. Thus, diffusion followed by wall recombination would be the main loss mechanisms for the O atom.

The extinction of the O atom in the afterglow is given by

$$\frac{dN(O)}{dt}=-\frac{N(O)}{\tau_d}-k_rN_n(O)N(x), \tag{3}$$

where $N(O)$ is the O atom density, $N(x)$ is the density of the main reaction species with O atoms, τ_d is the diffusion lifetime of the O atom, and k_r is the reaction rate constant between O atoms and reaction species. As shown in Fig. 9, the decay time constant of O atoms increases with the increase of O_2 pressure. The contribution of gas phase reaction to the loss reaction of O atoms is small as described above. Therefore, the term $k_rN_n(O)N(x)$ in Eq. (3) is negligible. Solving this rate equation, we have obtained a single exponential function for the decay of O atom concentration in afterglow plasma

$$N(O)=N_0(O)\exp(-t/\tau_d), \tag{4}$$

where $N_0(O)$ is the initial density of O atoms. Therefore, the measured decay time constant corresponds to the τ_d. This lifetime is well represented by the following equation:

$$\tau_d=\frac{p\Lambda_0^2}{D}+\frac{2l_0(2-\alpha)}{\nu\alpha}, \tag{5}$$

where p is pressure, D is the diffusion coefficient for O atoms in O_2, Λ_0 is the geometrical diffusion length determined by the chamber structure $[\Lambda_0^{-2}=(\pi/L)^2+(2.405/R)^2$: in the present study, height L is 30 cm and radius R is 20 cm], $l_0=V/S$ with the volume (V) band surface area (S) of the chamber, and ν is the velocity of O atoms given by $(8kT/\pi M)^{1/2}$ [T and M are temperature (300 K) and mass of O atoms, respectively, and k is Boltzmann constant]. α is the surface loss probability on the chamber wall. D was determined to be 2.9×10^4 cm^2 Pa/s. This value was derived from theoretical calculation (at 300 K) to be by the Chapman–Enskog theory with the Lennard-Jones intermolecular potential.[25,26] From this result, the surface loss probability on the stainless steel wall was decreased from 0.1 to 0.022 with increasing O_2 pressure. These results are almost the same order reported.[12] It has been reported that the surface reaction probability has a strong function of discharge conditions such as power, pressure, and the presence of ion bombardment. Moreover, the history of wall exposure to reactive gases could play a significant role in altering the surface reaction probability, even though the wall may nominally have the same composition.[23]

IV. DISCUSSION

We have developed a VUVAS system employing O_2 MHCL and established a measurement method for absolute O atom densities in process plasmas. The self absorption in the lamp was reduced by decreasing the O_2 partial pressure in the O_2 MHCL below 5.0 Pa. The background absorption for O_2 was evaluated employing the H_2 broad peak, since the absorptions using O line at 130.2 nm and H_2 broad peak at 128.5 nm showed similar behavior in the pressure range from 1.33 to 66.7 Pa. The line profile of O_2 MHCL was estimated to be a Voigt profile with $\Delta\nu_L/\Delta\nu_D=1.1$ at the O atom temperature of 300 K by means of a comparison between the measured absorption intensity and the theoretical absorption intensity as a function of rf power. This system has been applied to the determination of absolute O atom density in the processing plasma. Absolute O atom densities in the O_2 rf ICP were estimated to be on the order of 1×10^{12}–1×10^{13} cm^{-3}, when the O_2 pressure increased from 1.3 to 26.7 Pa at an ICP power of 100 W. The behavior of absolute O atom density employing the VUVAS technique was almost consistent with those obtained from the actinometry technique using 844.6 and 777.4 nm emission lines. This consistency indicated that the generation of excited O atoms by means of electron-impact dissociative excitation of the O_2

Downloaded 29 Oct 2006 to 133.6.32.11. Redistribution subject to AIP license or copyright, see http://rsi.aip.org/rsi/copyright.jsp

molecule due to a high-energy electron would be small under our conditions. Furthermore, the decay of the O atom density in O_2 afterglow plasma was measured. From this result, the decay curves of the O atom density were fitted well with single exponential functions, and decay time constant was larger for the lower gas pressure. The main loss mechanisms for the O atom would be diffusion followed by wall recombination. The surface loss probability on the stainless steel wall decreased from 0.1 to 0.022 with increasing O_2 pressure.

ACKNOWLEDGMENTS

The authors would like to thank Professor Akihiro Kono, Center for Cooperative Research in Advanced Science and Technology and Dr. Seigou Takashima, Nppon Laser & Electronics LAB for useful discussions.

[1] O. Joubert, J. Pelletier, and Y. Arnal, J. Appl. Phys. **65**, 5096 (1989).
[2] T. E. F. M. Standaert *et al.*, J. Vac. Sci. Technol. A **19**, 435 (2001).
[3] S. Panda, D. J. Economou, and L. Chan, J. Vac. Sci. Technol. A **19**, 398 (2001).
[4] K. Kim, M. H. An, Y. G. Shin, M. S. Suh, C. J. Youn, Y. H. Lee, K. B. Lee, and H. J. Lee, J. Vac. Sci. Technol. B **14**, 2667 (1996).
[5] T. Ueno, A. Morioka, S. Chikamura, and Y. Iwasaki, Jpn. J. Appl. Phys., Part 2 **39**, L327 (2000).
[6] M. Brake, J. Hinkle, J. Asmussen, M. Hawley, and R. Kerber, Plasma Chem. Plasma Process. **3**, 63 (1983).
[7] J. P. Booth and N. Sadeghi, J. Appl. Phys. **70**, 611 (1991).
[8] H. M. Katsch, A. Tewes, E. Quandt, A. Goehlich, T. Kawetzki, and H. F. Döbele, J. Appl. Phys. **88**, 6232 (2000).
[9] J. Amoorim, G. Baravian, M. Touzeau, and J. Jolly, J. Appl. Phys. **76**, 1487 (1994).
[10] E. J. Collart, J. A. G. Baggerman, and R. J. Visser, J. Appl. Phys. **78**, 47 (1995).
[11] R. E. Walkup, K. L. Saenger, and G. S. Selwyn, J. Chem. Phys. **84**, 2668 (1986).
[12] Angeliki D. Tserepi and T. A. Miller, J. Appl. Phys. **77**, 505 (1995).
[13] J. Matsushita, K. Sasaki, and K. Kadota, Jpn. J. Appl. Phys., Part 1 **36**, 4747 (1997).
[14] J. P. Booth, O. Joubert, J. Pelletier, and N. Sadeghi, J. Appl. Phys. **69**, 618 (1991).
[15] S. Takashima, M. Hori, T. Goto, A. Kono, M. Ito, and K. Yoneda, Appl. Phys. Lett. **75**, 3929 (1999).
[16] S. Takashima, S. Arai, A. Kono, M. Ito, K. Yoneda, M. Hori, and T. Goto, J. Vac. Sci. Technol. A **19**, 599 (2001).
[17] H. Nagai, S. Takashima, M. Hiramatsu, M. Hori, and T. Goto, J. Appl. Phys. **91**, 2615 (2002).
[18] S. Takashima, A. Kono, K. Yoneda, M. Hori, and T. Goto, J. Appl. Phys. **90**, 5497 (2001).
[19] K. Tachibana and H. Kamisugi, Appl. Phys. Lett. **74**, 2390 (1999).
[20] H. Ito, K. Teii, H. Funakoshi, M. Hori, T. Goto, M. Ito, and T. Takeo, J. Appl. Phys. **88**, 4537 (2000).
[21] H. Okabe, *Photochemistry of Small Molecules* (Wiley, New York, 1978).
[22] Y. Tanaka, J. Chem. Phys. **20**, 1728 (1952).
[23] H. Singh, J. W. Coburn, and D. B. Graves, J. Appl. Phys. **88**, 3748 (2000).
[24] Y. Kawai, K. Sasaki, and K. Kadota, Jpn. J. Appl. Phys., Part 2 **36**, L1261 (1997).
[25] R. C. Reid, J. M. Prausnitz, and T. K. Sherwood, *The Properties of Gases and Liquids* (McGraw–Hill, New York, 1977).
[26] R. A. Svehla, NASA Tech. Rep. No. R-132, 1962.

Downloaded 29 Oct 2006 to 133.6.32.11. Redistribution subject to AIP license or copyright, see http://rsi.aip.org/rsi/copyright.jsp